JACS
JOURNAL OF THE AMERICAN CHEMICAL SOCIETY
Communication
pubs.acs.org/JACS

Aziridinyl Fluorophores Demonstrate Bright Fluorescence and Superior Photostability by Effectively Inhibiting Twisted Intramolecular Charge Transfer

Xiaogang Liu,[*,†,‡,¶] Qinglong Qiao,[§,¶] Wenming Tian,[†] Wenjuan Liu,[†] Jie Chen,[†] Matthew J. Lang,[‡,⊥] and Zhaochao Xu[*,†]

[†]Key Laboratory of Separation Science for Analytical Chemistry, Dalian Institute of Chemical Physics, Chinese Academy of Sciences, 457 Zhongshan Road, Dalian 116023, China

[‡]Singapore-MIT Alliance for Research and Technology (SMART), 1 CREATE Way, Singapore 138602

[§]State Key Laboratory of Fine Chemicals, Dalian University of Technology, 2 Linggong Road, Dalian 116012, China

[⊥]Department of Chemical and Biomolecular Engineering and Department of Molecular Physiology and Biophysics, Vanderbilt University, Nashville, Tennessee 37235, United States

Supporting Information

ABSTRACT: Replacing conventional dialkylamino substituents with a three-membered aziridine ring in naphthalimide leads to significantly enhanced brightness and photostability by effectively suppressing twisted intramolecular charge transfer formation. This replacement is generalizable in other chemical families of fluorophores, such as coumarin, phthalimide, and nitrobenzoxadiazole dyes. In highly polar fluorophores, we show that aziridinyl dyes even outperform their azetidinyl analogues in aqueous solution. We also proposed one simple mechanism that can explain the vulnerability of quantum yield to hydrogen bond interactions in protonic solvents in various fluorophore families. Such knowledge is a critical step toward developing high-performance fluorophores for advanced fluorescence imaging.

Rapid evolution of fluorescence imaging techniques in recent years demands fluorophores with enhanced brightness and photostability.[1−4] This evolution, particularly in biomolecular labeling[5,6] and super-resolution imaging techniques,[7−10] has facilitated fluorescence imaging with single-molecule precision in numerous biological and biomedical studies.[11−13] However, many existing fluorophores lack sufficient brightness and photostability for single-molecule and live-cell imaging. Rational molecular engineering of fluorophores, based on a deep understanding of their working mechanism, is thus crucial and imperative to yield novel fluorophores with superior brightness and photostability.

On the theoretical side, it is proposed that twisted intramolecular charge transfer (TICT) acts as one of the major nonradiative de-excitation pathways in fluorophores.[14] In the TICT state, a dialkylamino donor twists out the fluorophore scaffold by approximately 90° upon photoexcitation, forming a non-emissive and highly reactive chemical species. Accordingly, various experimental strategies have been applied to avoid TICT formation. Commercially available fluorophores, such as Dylight, CF, and Alexa dyes, involve complex structural modifications by rigidifying amino substituents. Unfortunately, most molecular structures of these dyes are still not disclosed, constraining their further derivatization and functionalization. Song et al. employed a bulky 7-azabicyclo[2.2.1]heptane to replace commonly used dimethylamino substituents in rhodamine dyes.[15] This structural modification greatly improves the quantum yields and photostability of rhodamine dyes but at the cost of deteriorated water solubility. In a landmark paper, Lavis et al. changed *N*,*N*-dialkylamino substituents to four-membered azetidine rings in several chemical families of fluorophores, such as rhodamines, rhodols, and coumarins.[2] They demonstrated that the azetidine ring simultaneously improves dye brightness and photostability. Moreover, this simple structural modification retains biochemical properties of the parent compounds (such as cell permeability and intracellular labeling) and becomes accessible even in basic chemical synthesis laboratories. Nevertheless, the degree of improvement with the azetidine ring based approach varies across different fluorophore families. For instance, the quantum yield of azetidinyl naphthalimide is markedly lower than those of coumarins and rhodamines, demanding further improvement.[2] In this communication, we show that a three-membered aziridine ring suppresses TICT formation more effectively over the four-membered azetidine ring and other dialkylamino substituents; consequently, the aziridine ring leads to improved brightness and superior photostability in a range of fluorophores, in conjunction with enlarged Stokes shifts.

We initially chose naphthalimide-derived **1**−**7** as model compounds to investigate the effect of azacyclic substituents on minimizing TICT (Figure 1). Our computational studies show that the amino "arms" and the main fluorophore scaffold of **1**−**7** can align in three different conformations due to competing contributions from azacyclic strain energy, steric hindrance, and resonance effect (Figure 1a,b). The resonance effect depends on the electron-donating/withdrawing strength of both the azacyclic rings and the fluorophore scaffolds. We find that compounds **1**, **2**, and **3**−**7** possess the up−up, flat, and up−down

Received: April 16, 2016
Published: May 20, 2016

DOI: 10.1021/jacs.6b03924
J. Am. Chem. Soc. 2016, 138, 6960−6963

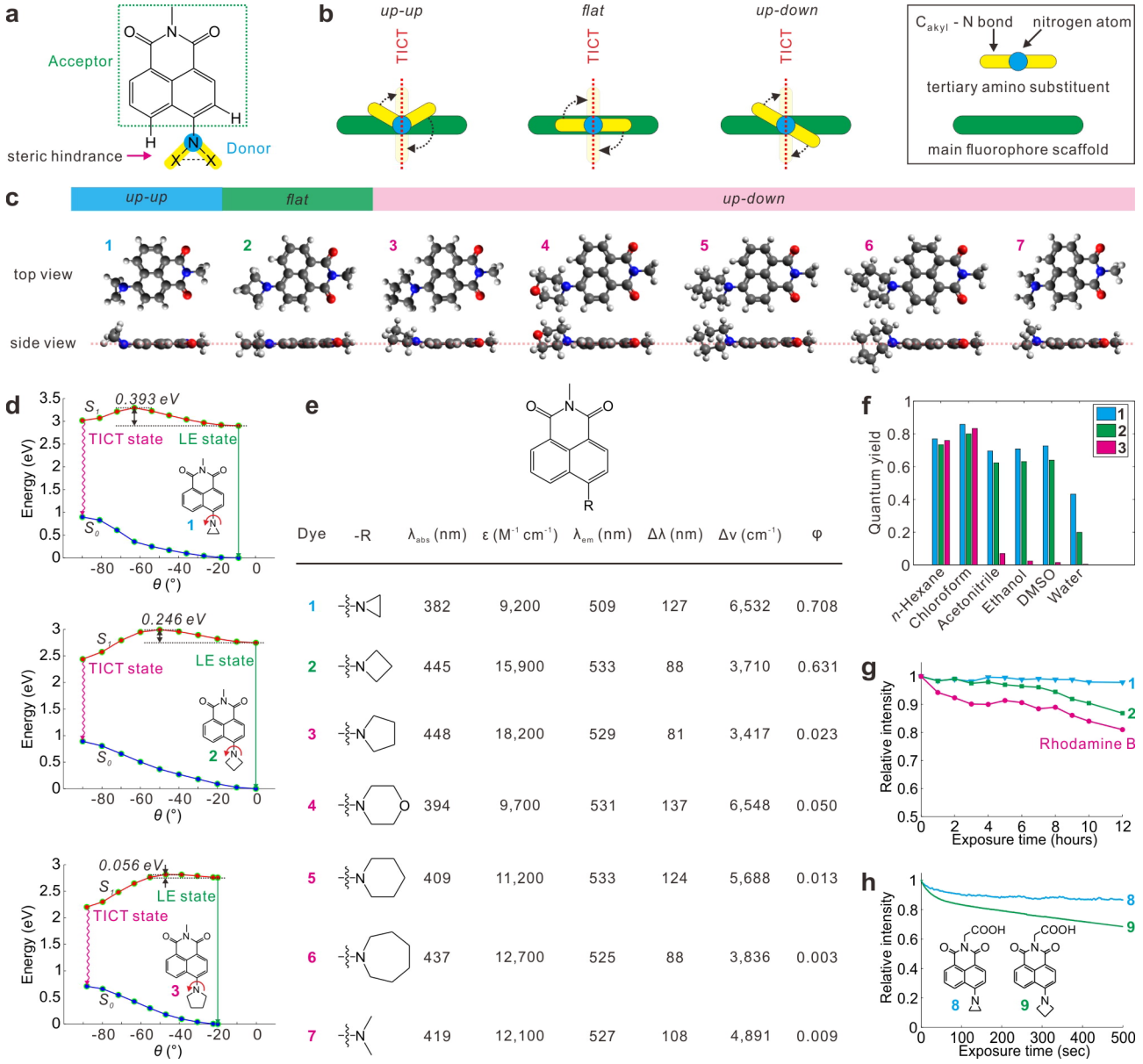

Figure 1. Three-membered aziridine ring enhances the brightness and photostability of naphthalimide fluorophores. (a) Illustration of steric hindrance between donor and acceptor moieties of a fluorophore. (b) Three types of alignment conformations between the two amino "arms" (highlighted in yellow) and the main fluorophore scaffold (green) in the ground state (S_0). Arrows indicate potential rotations to enter the TICT state in the first excited state (S_1). (c) Top and side views of the theoretically optimized molecular structures of **1**−**7** in ethanol in the ground state. (d) Calculated potential energy surfaces of the ground (S_0, in blue) and the first excited singlet (S_1, in red) states of **1**−**3** in ethanol, as a function of the rotational angle (θ) between the amino substituent and the main fluorophore scaffold. θ is the average dihedral angle of two amino arms with respect to the naphthalimide scaffold. The LE state has a more planar conformation and less charge transfer compared to the TICT state. (e) Experimental spectroscopic data for **1**−**7** in ethanol: λ_{abs}, peak UV−vis absorption wavelength; ε, molar extinction coefficient; λ_{em}, peak emission wavelength; $\Delta\lambda$ and $\Delta\nu$, Stokes shift; φ, quantum yield. (f) Experimental quantum yields of **1**−**3** in various solvents. (g) Relative intensity changes of **1**, **2**, and Rhodamine B in DMSO/water mixture (volume ratio, 30:70) during 12 h of strong white light exposure. (h) Relative intensity changes of **8** and **9** in water during 500 s of strong laser radiation (416 nm) in microfluidic channels. Insets show the molecular structures of **8** and **9**.

conformations, respectively (Figure 1c). Intuitively, the up−up conformation should possess the highest TICT resistance because one of its amino arms faces strong steric repulsion to enter the TICT state. Similarly, the up−down conformation should exhibit the lowest TICT resistance because steric hindrance facilitates its TICT rotation after photoexcitation.[16] Indeed, our theoretical calculations show that, in a polar environment (such as ethanol), the TICT state of **1** (the up−up conformation) is energetically unfavorable, and a significant energy barrier (0.393 eV) exists between the local excited (LE) and TICT states (Figure 1d). The TICT state of **2** (the flat conformation), however, becomes slightly more stable than the LE state, in conjunction with a reduced energy barrier (0.246 eV). In contrast, a strong tendency to the TICT state is most evident in **3** (the up−down conformation; Figure 1d). Nevertheless, in a nonpolar environment, our calculations show that **1**−**3** favor LE emission but not TICT rotation (Supporting Information section 1).

Experimental results are in excellent agreement with our theoretical calculations. In nonpolar solvents, **1**−**7** emit bright

DOI: 10.1021/jacs.6b03924
J. Am. Chem. Soc. 2016, 138, 6960−6963

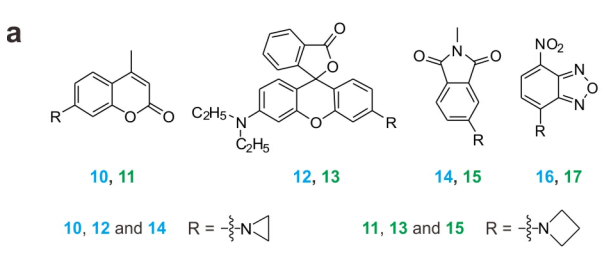

b

Dye	λ_{abs} (nm)	ε (M^{-1} cm^{-1})	λ_{em} (nm)	Δλ (nm)	Δν (cm^{-1})	φ
10	325	6,945	439	114	7,990	0.899
11	354	12,661	471	117	7,017	0.919
12	—	—	—	—	—	—
13	553	88,000	576	23	722	0.459
14	395	2,576	587	192	8,281	0.020
15	403	2,660	589	186	7,836	0.011
16	407	11,985	555	148	6,552	0.084
17	500	38,393	588	88	2,993	0.034

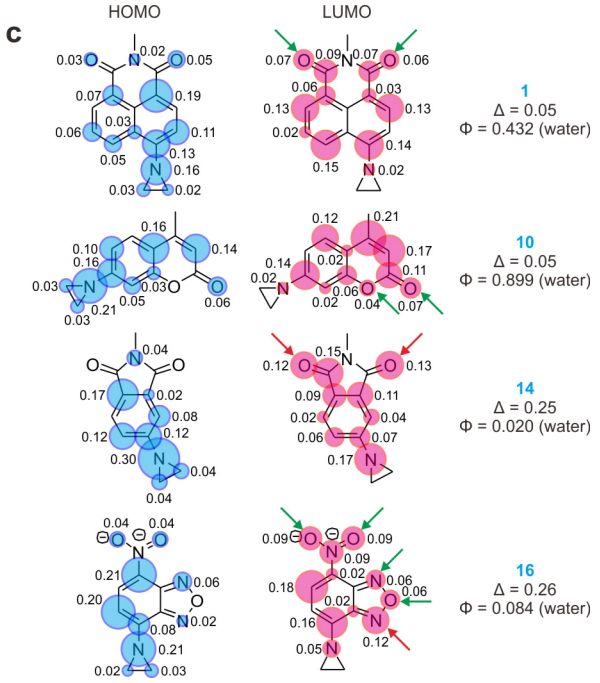

Figure 2. (a) Molecular structures of **10**–**17**. (b) Experimental spectroscopic data for **10**–**17** in aqueous solution: λ_{abs}, peak UV–vis absorption wavelength; ε, molar extinction coefficient; λ_{em}, peak emission wavelength; $\Delta\lambda$ and $\Delta\nu$, Stokes shift; φ, quantum yield. (c) Atomic contributions to the HOMO (highest occupied molecular orbital) and LUMO (lowest unoccupied molecular orbital) electron densities of **1**, **10**, **14**, and **16**, calculated based on the optimized molecular structures in the S_0 state. The blue/pink circle size represents the atomic contribution; only contributions >0.02 are shown. Hydrogen bond formation sites in naphthalimide, coumarin, phthalimide, and NBD fluorophore scaffolds are indicated by arrows. Molecular sites that experience significant partial charge increase upon photoexcitation are highlighted by red arrows in **14** and **16**.

fluorescence (quantum yield, $\varphi \approx 0.750$). In polar solvents, only **1** and **2** demonstrate high quantum yields. We notice that **1** exhibits quantum yields higher than those of **2** in all tested solvents. This difference is most apparent in water ($\varphi = 0.432$ for **1** and 0.199 for **2**; Figure 1e,f; Supporting Information section 2). It is thus clear that the aziridine ring possesses higher TICT resistance than the azetidine ring and other dialkylamino substituents.

We then tested the photostability of **1** and **2** (under white light radiation; Figure 1g) and their analogues with enhanced water solubility, **8** and **9** (under 416 nm laser radiation; Figure 1h). Our tests show that aziridinyls **1** and **8** exhibit photostability considerably higher than that of azetidinyls **2** and **9**. The chemical stability of **1** was also evaluated in solutions of different pH. We found that the fluorescence intensities of **1** remained stable from pH 4.2 to 10.8. We also treated the solution of **1** with various metal ions, oxidants, and nucleophiles including H_2O_2, NaHS, cysteine, and glutathione. The unperturbed emission indicates that **1** has good chemical stability (Supporting Information section 2).

Several other differences between **1** and **2** are of note. The up–up conformation of **1** yields a lower molar extinction coefficient and a blue shift in its UV–vis absorption peak (ε = 9200 M^{-1} cm^{-1} and λ_{abs} = 382 nm) with respect to the planar **2** (ε = 15 900 M^{-1} cm^{-1} and λ_{abs} = 445 nm; Figure 1e). This is due to a poorer resonance effect in **1**. However, a slight flattening of the aziridine ring in **1** upon photoexcitation results in a large geometry relaxation in the excited state, thus leading to a favorable large Stokes shift ($\Delta\lambda$ = 127 nm for **1** vs 88 nm for **2**).[17] The large Stokes shift of **1** is "indispensable in multicolor super-resolution techniques".[18] Moreover, due to the larger quantum yield of **1**, its brightness is ~27% higher than that of **2** in aqueous solution. The same patterns were observed between **8** and **9** (Supporting Information section 2).

Inspired by the improved brightness, enhanced stability, and enlarged Stokes shifts in naphthalimide dyes, we then employed the aziridine ring in coumarin, rhodamine, phthalimide, and nitrobenzoxadiazole (NBD) dyes and compared the fluorophore performance against that of their azetidinyl and dimethylamino analogues (Figure 2a,b). Our quantum chemical calculations show that aziridinyl fluorophores demonstrate the highest TICT resistance followed by azetidinyl dyes. Experimental data also show that both aziridinyl and azetidinyl fluorophores exhibit higher brightness than conventional dialkylamino fluorophores (φ = 0.058 for coumarin 1; <0.01 for dimethylamino NBD and phthalimide in water). Between aziridinyl and azetidinyl fluorophores, coumarins **10** and **11** display comparably high quantum yields ($\varphi \approx 0.900$) in water. Since these 4-methylcoumarin dyes have a low polarity and weak TICT tendency, the azetidine ring seems sufficient to suppress TICT formation and afford high quantum yields. The aziridine substituent in **12** leads to the colorless and nonfluorescent lactone form of rhodamine dyes, while azetidinyl **13** is highly emissive (φ = 0.459). These results are consistent with Lavis and co-workers' observations on similar rhodamine dyes, where both dialkylamino groups are replaced by aziridine or azetidine rings.[2] In contrast, for phthalimide and NBD dyes **14**–**17**, the quantum yields of aziridinyl fluorophores are approximately twice as large as those of azetidinyl analogues in aqueous solution, in conjunction with enlarged Stokes shifts (Figure 2b). These results are remarkable, considering that dimethylamino phthalimide and NBD dyes are non-emissive in water.[19,20] Unfortunately, the absolute quantum yields of **14**–**17** (φ =

DOI: 10.1021/jacs.6b03924
J. Am. Chem. Soc. 2016, 138, 6960–6963

0.011−0.084) are low, largely due to intensive hydrogen bond interactions around the fluorophore scaffolds.[19,21]

We have found one plausible mechanism to explain the vulnerabilities of quantum yield to hydrogen bond interactions among different fluorophores. This vulnerability is closely related to the partial charge increase upon photoexcitation at hydrogen bond formation sites in the fluorophore scaffolds (Figure 2c, highlighted by arrows). We denote the total charge change at these sites during HOMO → LUMO transition as Δ. In naphthalimide and coumarin dyes, no significant Δ changes are observed. Coincidentally, the quantum yields of **1** and **10** are high (φ = 0.432 for **1** and 0.899 for **10**). In contrast, we notice substantial Δ increases in phthalimide and NBD dyes **14** and **16** (Figure 2c, highlight by red arrows), indicating intensive hydrogen bond interactions after photoexcitation. Accordingly, their quantum yields are low (φ = 0.020 for **14** and 0.084 for **16**). Interestingly, this mechanism also works perfectly in explaining the quantum yield differences of several other fluorophore families in protonic solvents, such as rhodol and oxazine dyes (Supporting Information section 1). Additional quantum chemical calculations including explicit solvent molecules are required to further understand such hydrogen bond interactions and are the subject of future work.

In conclusion, we have demonstrated that the up−up conformed aziridine ring is highly effective in suppressing TICT rotation. Aziridinyl fluorophores thus demonstrate considerably enhanced brightness and superior photostability in comparison to that in conventional dialkylamino substituted dyes. In highly polar fluorophores with a strong TICT tendency (such as naphthalimide dyes), aziridinyl fluorophores even outperform their azetidinyl analogues in aqueous solution. As another favorable feature, a slight flattering of the aziridine ring upon photoexcitation affords large Stokes shifts in aziridinyl fluorophores. Moreover, similar to that of the azetidine ring, employing the aziridine ring requires minimal structural modifications, retains advantages of the parent fluorophores, permits facile synthesis and further derivatization, and can be applied to a wide range of fluorophores to enhance dye brightness and photostability. Finally, we show that substantial charge increase at hydrogen bond formation sites in a fluorophore is detrimental to its quantum yield in protonic solvents. Such knowledge on controlling TICT and managing hydrogen bond interactions will inspire the rational development of abundant high-performance dyes across different fluorophore families, thus enabling unprecedented fluorescence imaging applications.

■ ASSOCIATED CONTENT

Supporting Information

The Supporting Information is available free of charge on the ACS Publications website at DOI: 10.1021/jacs.6b03924.

Synthesis, characterization, and computational details (PDF)

■ AUTHOR INFORMATION

Corresponding Authors

*xiaogang@smart.mit.edu.

*zcxu@dicp.ac.cn.

Author Contributions

¶X.L. and Q.Q. contributed equally to this work.

Notes

The authors declare no competing financial interest.

■ ACKNOWLEDGMENTS

X.L. and M.J.L. thank the National Research Foundation of Singapore (through BioSyM Interdisciplinary Research Group at Singapore-MIT Alliance for Research and Technology) for supporting this project. Z.X. acknowledges the National Natural Science Foundation of China (21276251), the 100 Talents Program funded by Chinese Academy of Sciences, Dalian Cultivation Fund for Distinguished Young Scholars (2014J11JH130 and 2015J12JH205), and the National Science Fund for Excellent Young Scholars (21422606). The authors thank Dr. Jie Pan for her assistance with photostability tests.

■ REFERENCES

(1) van der Velde, J. H.; Oelerich, J.; Huang, J.; Smit, J. H.; Jazi, A. A.; Galiani, S.; Kolmakov, K.; Guoridis, G.; Eggeling, C.; Herrmann, A.; et al. *Nat. Commun.* **2016**, *7*, 10144.

(2) Grimm, J. B.; English, B. P.; Chen, J.; Slaughter, J. P.; Zhang, Z.; Revyakin, A.; Patel, R.; Macklin, J. J.; Normanno, D.; Singer, R. H.; Lionnet, T.; Lavis, L. D. *Nat. Methods* **2015**, *12*, 244.

(3) Dempsey, G. T.; Vaughan, J. C.; Chen, K. H.; Bates, M.; Zhuang, X. *Nat. Methods* **2011**, *8*, 1027.

(4) Altman, R. B.; Terry, D. S.; Zhou, Z.; Zheng, Q.; Geggier, P.; Kolster, R. A.; Zhao, Y.; Javitch, J. A.; Warren, J. D.; Blanchard, S. C. *Nat. Methods* **2012**, *9*, 68.

(5) Gautier, A.; Juillerat, A.; Heinis, C.; Corrêa, I. R.; Kindermann, M.; Beaufils, F.; Johnsson, K. *Chem. Biol.* **2008**, *15*, 128.

(6) Los, G. V.; Encell, L. P.; McDougall, M. G.; Hartzell, D. D.; Karassina, N.; Zimprich, C.; Wood, M. G.; Learish, R.; Ohana, R. F.; Urh, M.; et al. *ACS Chem. Biol.* **2008**, *3*, 373.

(7) Planchon, T. A.; Gao, L.; Milkie, D. E.; Davidson, M. W.; Galbraith, J. A.; Galbraith, C. G.; Betzig, E. *Nat. Methods* **2011**, *8*, 417.

(8) Jones, S. A.; Shim, S.-H.; He, J.; Zhuang, X. *Nat. Methods* **2011**, *8*, 499.

(9) Huang, B.; Babcock, H.; Zhuang, X. *Cell* **2010**, *143*, 1047.

(10) Huang, B.; Bates, M.; Zhuang, X. *Annu. Rev. Biochem.* **2009**, *78*, 993.

(11) Lukinavičius, G.; Umezawa, K.; Olivier, N.; Honigmann, A.; Yang, G.; Plass, T.; Mueller, V.; Reymond, L.; Corrêa, I. R., Jr.; Luo, Z.-G.; et al. *Nat. Chem.* **2013**, *5*, 132.

(12) Jungmann, R.; Avendaño, M. S.; Dai, M.; Woehrstein, J. B.; Agasti, S. S.; Feiger, Z.; Rodal, A.; Yin, P. *Nat. Methods* **2016**, *13*, 439.

(13) Legant, W. R.; Shao, L.; Grimm, J. B.; Brown, T. A.; Milkie, D. E.; Avants, B. B.; Lavis, L. D.; Betzig, E. *Nat. Methods* **2016**, *13*, 359.

(14) Grabowski, Z. R.; Rotkiewicz, K.; Rettig, W. *Chem. Rev.* **2003**, *103*, 3899.

(15) Song, X.; Johnson, A.; Foley, J. *J. Am. Chem. Soc.* **2008**, *130*, 17652.

(16) Vogel, M.; Rettig, W.; Sens, R.; Drexhage, K. H. *Chem. Phys. Lett.* **1988**, *147*, 452.

(17) Liu, X.; Xu, Z.; Cole, J. M. *J. Phys. Chem. C* **2013**, *117*, 16584.

(18) Sednev, M. V.; Belov, V. N.; Hell, S. W. *Methods Appl. Fluoresc.* **2015**, *3*, 042004.

(19) Loving, G.; Imperiali, B. *J. Am. Chem. Soc.* **2008**, *130*, 13630.

(20) Saha, S.; Samanta, A. *J. Phys. Chem. A* **1998**, *102*, 7903.

(21) Vázquez, M. E.; Blanco, J. B.; Imperiali, B. *J. Am. Chem. Soc.* **2005**, *127*, 1300.

DOI: 10.1021/jacs.6b03924
J. Am. Chem. Soc. 2016, 138, 6960−6963